Polym. Bull. (2019) 76:447–467
https://doi.org/10.1007/s00289-018-2375-1

ORIGINAL PAPER

Synthesis of multiblock linear polyether functional amino silicone softener and its modification of surface properties on cotton fabrics

Yuan Wei[1] · Cheng Zheng[1] · Peng Chen[1] · Qiming Yu[2] · Taoyan Mao[1] · Jing Lin[1] · Liqiang Liu[1]

Received: 9 September 2017 / Revised: 12 May 2018 / Accepted: 15 May 2018 /
Published online: 7 June 2018

Abstract Multiblock copolymers of polyether-modified amino silicone softener (ETSO-PEA) were successfully synthesized with epoxy-terminated polysiloxane (ETSO) and polyether amine. The chemical structure of ETSO-PEA was characterized by ^{1}H NMR, FTIR and TGA. Single-factor and orthogonal array design experiments affecting the conversion rate of product were carried out to investigate the optimal reaction conditions. In the first two steps, the data between viscosity/conversion rate and reaction time showed that the two steps were both kinetic first-scale reaction. The application of ETSO-PEA used as softener on cotton fabrics was studied. The results showed that the ETSO-PEA-treated cotton fabrics expressed better hydrophilicity, wettability and whiteness than traditional amino silicone softener-treated samples. The morphology images indicated that the scales and clearance on the surface of the untreated cotton fibers were covered with a smooth film after treating with the silicones solution. Amino silicone softener was fixed onto the cotton fabrics, and the surface was modified with a formation of network structure. Meanwhile, the extent of networking and crosslinking was enhanced a lot, which provided a good soft handle. The polyether segment with less bending on the ETSO-PEA disrupted the continuous arrangement of Si–CH_3 groups and limited the movement of polysiloxane segment, giving the cotton fabric a better hydrophilic and slightly rougher surface than ATSO-treated samples. This work provided an optimized and

Electronic supplementary material The online version of this article (https://doi.org/10.1007/s00289-018-2375-1) contains supplementary material, which is available to authorized users.

✉ Cheng Zheng
1912730783@qq.com

[1] Department of Chemical Engineering, Guangzhou University, Guangzhou 510006, People's Republic of China

[2] Griffith School of Engineering, Griffith University, Brisbane, QLD 4111, Australia

cost-effective method to synthesize high-performance multiblock polyether functional amino silicone softener.

Keywords Silicone softener · Hydrophilicity · Whiteness · Morphology · Kinetics

Introduction

Silicone softeners have played a very important role in final finishing. In daily life, a piece of fabric product without a good handle is almost impossible to be appealing to the public. Therefore, silicone softeners are widely used to turn rough fabrics into soft textiles [1, 2]. High-quality fabrics have been favored by everyone, and buyers can enjoy a perfect wearing comfort. There are two conventional methods in the synthesis of functional polysiloxanes: hydrosilylation among polysiloxanes and compounds containing double bonds, as well as hydrolysis and condensation polymerization of siloxane with silane coupling agents [3–6]. Silicones are special and functional materials that can affect the basic properties of fabrics such as softness, hydrophilicity, wettability and anti-wrinkle properties [7–9].

Amino silicones have excellent ability to form a film on the fabrics [10–12]. It was observed that the film forming on the surface of fabrics could reduce the friction factor and minimize the gap between the wool scales, which increased surface smoothness [1, 13]. This morphology can affect the mechanical properties of the surface of the fabrics, and the relevant film-forming mechanism has become a hot spot in recent research [14, 15].

Over a long period in the past, there were some commonly used traditional softeners (such as *N*-γ-aminopropylpolysiloxane and *N*-β-aminoethyl-γ-aminopropylpolysiloxane) in the market, which could increase the softness and handle. However, the treated cotton fabrics were prone to yellowing in the course of use, also with a worse hydrophilicity. The result is that light-colored fabrics turn yellow and off shade. In the presence of amino compounds, air and heat or light can result in the yellowing because of the oxidation of amino radicals [16–19]. Therefore, on the basis of maintaining the excellent soft and smooth properties of the amino silicones, the appropriate reduction of the amine value will help to reduce the yellowing.

In addition, consumers' attitude toward a comfortable and active lifestyle in recent years has created a rapidly increasing market for functional textiles. It has become more important to develop novel amino silicones to replace the traditional amino silicone products. They should improve fabrics with excellent softness, whiteness, hydrophilicity and wettability. All kinds of modified silicones have been designed and synthesized to satisfy people's needs. For example, it was studied that secondary/tertiary amine or low amine value-modified silicones can give cotton fabrics better whiteness [20, 21]. It was found that polyether-grafted/blocked polysiloxanes, which contained hydrophilic chains (polyether), could impact cotton fabrics with excellent hydrophilicity [22–26]. Keeping in mind that background, silicones with functional groups should be applied to the molecular structure design.

In this study, a linear functional silicone softener-containing polyether was synthesized by using a three-step reaction pathway. First, hydrogen-terminated polysiloxane (HTSO) was synthesized by a ring-opening polymerization reaction between octamethyl cyclotetrasiloxane (D4) and 1,1,3,3-tetramethyldisiloxane. Then, it reacted with allyl glycidyl ether (AGE) via hydrosilylation to obtain epoxy-terminated polysiloxane (ETSO). ETSO further reacted with polyether amine (ED-600 and T-403) to produce polyether amine-modified polysiloxane (ETSO-PEA). The ETSO-PEA-treated cotton fabrics expressed good performance properties, and compared with traditional amino siloxane, they also maintained good wettability and hydrophilicity.

Experimental

Materials and methods

Octamethyl cyclotetrasiloxane (D4) was obtained from Dow Corning. 1,1,3,3-Tetramethyldisiloxane was obtained from Hongfu Silicone Co., Ltd (China). Allyl glycidyl ether was provided by Nanjing Royal Monte Chemical Co., Ltd (China). Sulfuric acid and AEO-7 were obtained from Guangzhou Chemical Co., Ltd (China). Chloroplatinic acid and Speier catalyst were provided by Aladdin Reagent. Two amino-terminated polyethers (ED600 and T-403) were provided by Huntsman Chemical Co., Ltd (China). Ammonia propyl terminated polysiloxane (ATSO) was provided by Qingyuan Hongtu Auxiliary Co., Ltd (China). Acetic acid (HAc) was provided by Tianjin Damao Chemical Co., Ltd (China). All reaction solvents were analytical reagents and used without further purification.

Synthesis process of HTSO, ETSO and ETSO-PEA

The synthesis process included three steps (Scheme 1). The single-factor and orthogonal optimization experiments were carried out to investigate the optimal reaction conditions in the first two steps.

Step 1: A mixture of D4 (1,1,3,3-tetramethyldisiloxane) and H_2SO_4 was added into a three-necked flask (250 mL) equipped with a stirring apparatus, thermometer and condenser to react for 8 h at a temperature of 40 °C and under the protection of nitrogen atmosphere. After that, Na_2CO_3 was dropped to neutralize the solution for 1 h. The crude product was filtered and vacuum-distilled to remove contained unreacted monomers and smaller molecule products to obtain a clear and transparent viscous liquid [hydrogen-terminated polysiloxane (noted as HTSO)].

Step 2: To a three-necked flask, equipped with a reflux condenser, a thermometer and a nitrogen inlet tube, a mixture of hydrogen-terminated polysiloxane and AGE was added, with chloroplatinic acid as Speier catalyst. The reaction mixture was maintained at 120 °C for 3 h. After the low-boiling-point impurities were removed under reduced pressure for 30 min at 100 °C, a colorless transparent liquid [epoxy-terminated polysiloxane (noted as ETSO)] was obtained.

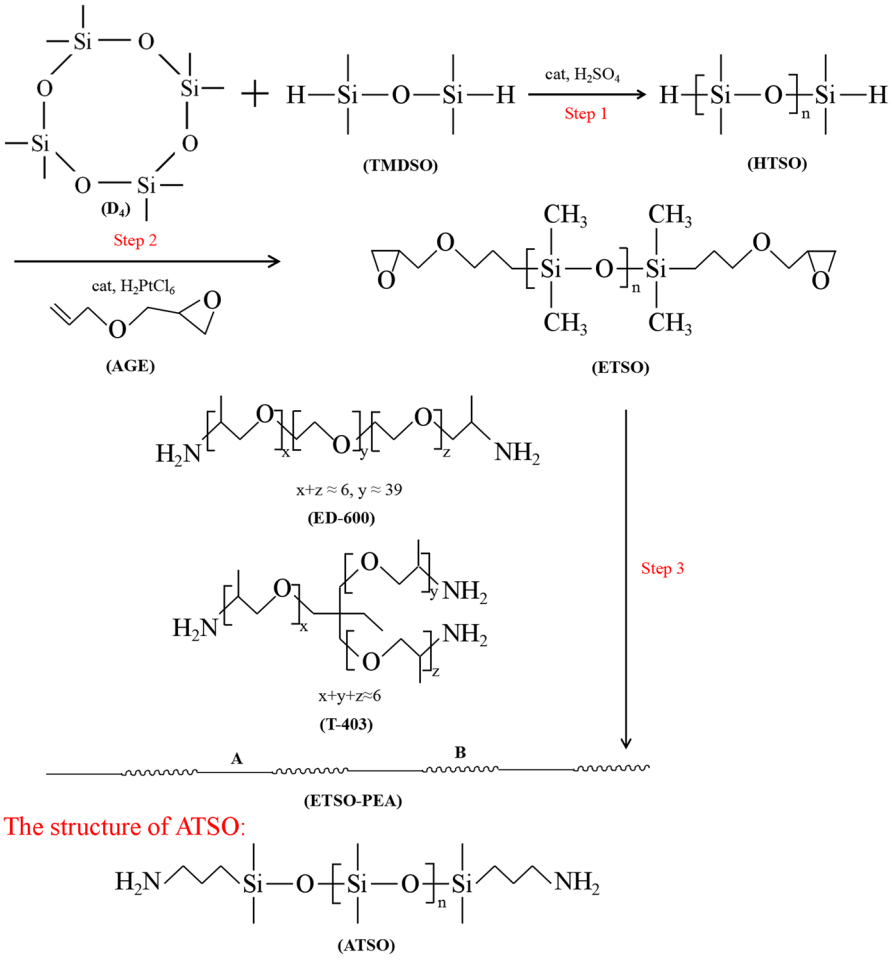

Scheme 1 Synthesis route of ETSO-PEA

Step 3: Similar to step 2, a mixture of as-prepared ETSO, ED 600 (4 g) and glacial acetic acid (3 g) was added and dissolved in isopropanol (40 wt%) at 83 °C. After this process, another polyether amine T-403 (3.4 g) was added to continue to react for another 8 h. Finally, a light yellow transparent liquid [polyether amine-modified polysiloxane (noted as ETSO-PEA, designed Mn = 10000 g/mol, determined by chemical titration method)] was obtained.

A traditional amino silicone, ATSO (shown in Scheme 1, designed Mn = 20000 g/mol, determined by chemical titration method), which has a similar but different functional chemical structure from ETSO-PEA, was used to compare with the product ETSO-PEA in the fabrics treatment.

Single-factor and orthogonal array design

In this study, the experiments carried out were based on an orthogonal array experimental design where three variables were analyzed as follows: reaction temperature, reaction time and catalyst concentration. The three variables were identified to have larger effects on the yield of the intermediate product. Thus, we chose an orthogonal array of three factors and three levels to assign the considered factors and levels [27].

According to the orthogonal array, nine trials were carried out to complete the optimization process in each reaction step. Through the range analysis, data analysis was carried out to reflect the magnitude of each factor and determine the optimal reaction conditions.

Treatment process

The fabrics should be treated with ETSO-PEA emulsion, which was prepared by the method of phase inversion emulsification [28, 29]. To a conical flask, ETSO-PEA (3 g) and AEO-7 (0.5 g, nonionic emulsifier) were mixed and stirred for 20 min. And then, 10 wt% HAc solution (10 g) was added in drops, which was helpful to form a uniform and transparent water-in-oil silicone emulsion. Lastly, water (87 g) was added successively to prepare oil-in-water emulsion [16, 30].

The pre-weighted raw fabrics were soaked in the silicone emulsion (weight ratio, fabrics/bath = 1:10) for 10 min and then padded. Finally, the padded fabrics were dried at 100 °C for 120 s and cured at 180 °C for 90 s. Then, they were kept in a dry container to balance for 24 h (noted as ETSO-PEA/cot).

Testing methods

Molecular structure

^{1}H NMR spectra were obtained on a AV III, Ascend 500 MHz Bruker NMR spectrometer using $CDCl_3$ as solvent. FTIR spectra were recorded on a Bruker Model Tensor 27 spectrometer using KBr for tableting. The scanning range was from 4000 to 400 cm^{-1} with a resolution of 0.4 cm^{-1}.

The degree of polymerization of the amino silicone oil can be characterized by viscosity, which was an easy way to show the length of siloxane backbone in the amino silicone [31, 32]. A higher viscosity indicates a longer siloxane backbone formed and a higher degree of polymerization reacted. In this study, the viscosity was measured with NDJ-5S digital viscometer. The conversion rate of ETSO was determined by the method of chemical titration.

Properties of treated cotton fabrics

Whiteness (expressed as whiteness index), hydrophilicity [static water contact angle (WCA)] and softness [bending rigidity (BR)] of treated cotton fabrics were

measured by WSB-2 digital whiteness meter, JC 2000C static contact angle measurement instrument and LLY-01B electric rigidity tester, respectively. TGA measurements were taken under air atmosphere with thermogravimetric analyzer Perkin Elmer TGA 4000 (heating rate = 20 °C/min; scan range = 50–500 °C) [33].

Surface morphology of cotton fabrics

Surface morphology of silicones-treated cotton fabrics was studied by scanning electron microscope, which was conducted on Phenom ProX SEM at an accelerating voltage of 10 kV. Before scanning, the treated/untreated cotton fabrics were coated with gold under vacuum conditions.

Results and discussion

Optimization of HTSO characteristics

The reaction results of each factor are shown in Fig. 1a–c. Based on the change in the result value of each factor, it can be found that the reaction temperature seems to have had little effect on the viscosity when it was increased to 40 °C, with a change from 242.2 to 241.6 mPa s. The viscosity increased from 214.2 to 239.5 mPa s, with the catalyst concentration rate increasing from 1 to 3%. As for reaction time, the viscosity increased sharply and reached a maximum at 8 h. It had a great effect on the viscosity, with a large change from 47.3 to 241.1 mPa s. More than this, it was observed that some more viscous by-products appeared at the bottom of the reaction vessel when the reaction temperature was above 50 °C.

According to the orthogonal array of three factors and three levels, nine experiments were designed and their values of viscosity are given in Table 1. It shows that the range of the viscosity varies from 192.3 to 240.9 mPa s; these original data of reaction results were recorded and used in the following range analysis.

About range analysis, two important parameters should be mentioned: K_i and R_i. K_i was defined as the sum of the evaluation indexes of the three levels ($i = 1, 2, 3$) in each factor and $\bar{K}_i$ (the mean value of K_i) was used to obtain the optimal combination of factors and levels. R_j (j = A, B, C) reflected the numerical gap between the maximum and minimum value of $\bar{K}_i$ and evaluated the importance of each factor [27].

The values of $\bar{K}_i$ in the range analysis are also listed in Table 1. For the data, a higher value ($\bar{K}_i$) indicates that the single level effects the viscosity results larger. Based on Table 1, the largest viscosity for each level was observed at reaction time 10 h (228.3 mPa s), reaction temperature 50 °C (233.8 mPa s) and catalyst concentration 2.5 wt% (231.3 mPa s), since K_i was the largest at this combination ($A_2B_3C_3$). As it was mentioned, a larger R_i indicates that the factor has a larger impact on the viscosity results. Therefore, compared with the values (R_i) of different factors, the significance of each factor was listed as follows: catalyst concentration rate (24.1) > reaction temperature (23.2) > reaction time (10.4). The range value R_C

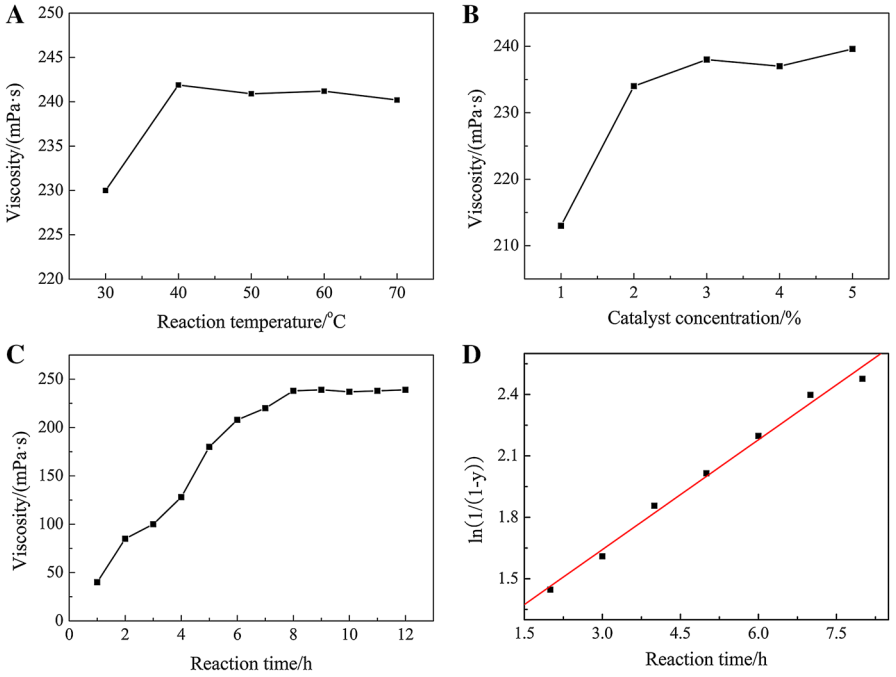

Fig. 1 Effect of single reaction factors on viscosity of HTSO, **a** reaction temperature; **b** catalyst concentration; **c** reaction time; **d** the relationship between "$\ln[1/(1-y)]$" and time

Table 1 Results of orthogonal experiments of HTSO characteristics

Trial no.	Factor levels			Results (Y_i) Viscosity (mPa s)
	Reaction temperature A (°C)	Reaction time B (h)	Catalyst concentration C (wt%)	
1	30	6	1.5	192.3
2	30	8	2	211.7
3	30	10	2.5	227.8
4	40	6	2	235.1
5	40	8	2.5	240.9
6	40	10	1.5	225.4
7	50	6	2.5	225.3
8	50	8	1.5	204.1
9	50	10	2	231.8
K_1	631.8	652.7	621.8	
K_2	701.4	656.7	678.6	
K_3	661.2	685.0	694.0	
$\bar{K}_1$	210.6	217.6	207.3	
$\bar{K}_2$	233.8	218.9	226.2	
$\bar{K}_3$	220.4	228.3	231.3	
R_j	23.2	10.4	24.1	

and R_A are larger, which reflects that a small change in these two factors can make a significant change in the viscosity of HTSO.

Optimization of ETSO characteristics

The reaction results of each factor are shown in Fig. 2a–c. Based on the change in the mean value of each factor, it can be observed that conversion rate of ETSO steadily increased from 76.4 to 94.0%, with the reaction temperature increasing from 90 to 140 °C. The catalyst concentration had a large effect on the conversion rate when it was increased to 30 ppm, with a change from 87.8 to 93.6%. As for reaction time, the conversion rate increased sharply and reached a maximum at 3 h, with a change from 72.2 to 93.6%.

Similar to the previous section of 3.1, the orthogonal array of three factors (reaction time, temperature and catalyst concentration) and three levels were carried out and their conversion rates are given in Table 2. Compared with the values (R_i) of different factors, the significance of each factor was listed as follows: reaction time (2.1) > catalyst concentration (2.0) > reaction temperature (0.6). So, the reaction time and catalyst concentration are observed to have a significant effect on the conversion rate of the product. The relationship of each factor level was shown as: $A_2 > A_3 > A_1$, $B_2 > B_3 > B_1$, $C_3 > C_2 > C_1$, which indicates that the best combination was $A_2B_2C_3$.

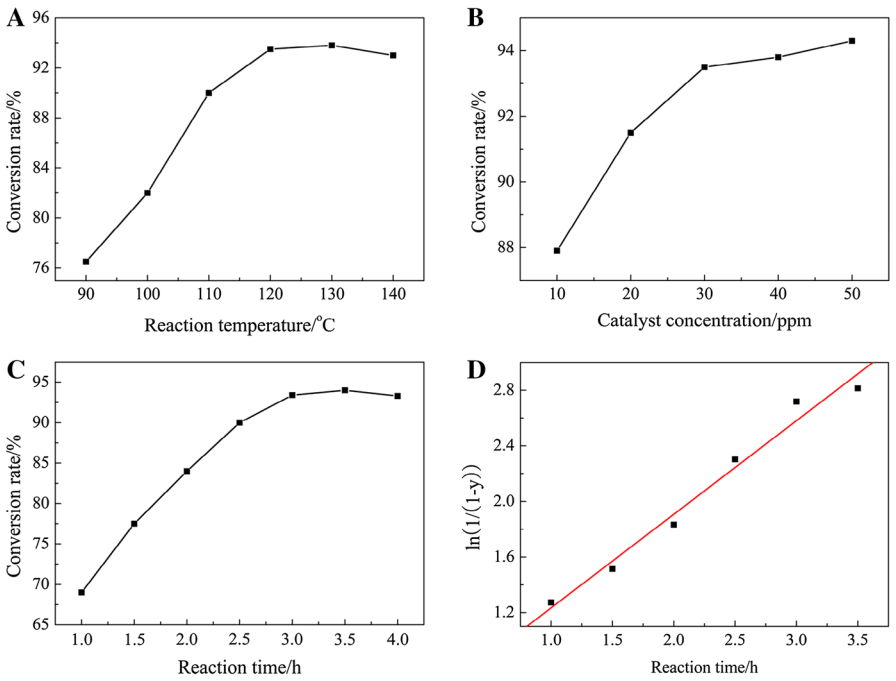

Fig. 2 Effect of single reaction factors on conversion rate of ETSO, **a** reaction temperature; **b** catalyst concentration; **c** reaction time; **d** the relationship between "ln[1/(1 − *y*)]" and time

Table 2 Results of orthogonal experiments of ETSO characteristics

Trial no.	Factor levels			Results (Y_i) Conversion rate (%)
	Reaction temperature A (°C)	Reaction time B (h)	Catalyst concentration C (ppm)	
1	110	2	10	87.7
2	110	3	20	91.5
3	110	4	30	92.1
4	120	2	10	90.4
5	120	3	30	92.3
6	120	4	10	90.2
7	130	2	30	90.4
8	130	3	10	91.0
9	130	4	20	90.9
K_1	271.3	268.5	268.9	
K_2	272.9	274.8	272.8	
K_3	272.3	273.2	274.8	
$\bar{K}_1$	90.4	89.5	89.6	
$\bar{K}_2$	91.0	91.6	90.9	
$\bar{K}_3$	90.8	91.1	91.6	
R_j	0.6	2.1	2.0	

Study on kinetics of the reaction

Study on kinetics of HTSO characteristics

In the synthesis of HTSO, a study on the kinetics was carried out by determining the change in conversion rate of product with reaction time (Fig. 1d). Firstly, the conversion rate of the reaction was calculated approximately by the data of viscosity:

$$y = \frac{\mu_t - \mu_0}{\mu_t}$$

where y: conversion rate, %; μ_t: viscosity at the time of t, mPa s; μ_0: initial viscosity, mPa s.

Then, the integral method was used to determine the reaction order. It was assumed that the reaction was a first-order reaction and the experimental data were integrated into the integral formula of the first-order reaction:

$$\ln \frac{1}{1-y} = kt$$

where y: conversion rate, %; k: rate coefficient, h^{-1}.

There has been basically a linear relationship between "ln[1/(1 − y)]" and time, which indicates that the rate constant is a constant ($k_1 = 0.18$). Thus, the hypothesis has been proved to be correct and the kinetic equation was:

$$r_1 = 0.18\,[A_1]$$

where r_1: chemical reaction rate, mol/dm^3 s; A_1: the concentration of HTSO at the time of t.

Study on kinetics of ETSO characteristics

Similar to the 3.3.1, a study on the kinetics of ETSO characteristics was carried out by determining the change in conversion rate of ETSO with reaction time (Fig. 2d). Furthermore, the integral method was used to determine the reaction order. It was assumed that the reaction was a first-order reaction and the experimental data were integrated into the integral formula of the first-order reaction:

$$\ln \frac{1}{1-y} = kt$$

where y: conversion rate, %; k: rate coefficient, h^{-1}.

There has been basically a linear relationship between "ln[1/(1 − y)]" and time, which indicates that the rate constant is a constant ($k = 0.67$). Thus, the hypothesis has been proved to be correct and the kinetic equation was:

$$r_2 = 0.67\,[A_2]$$

where r_2: chemical reaction rate, mol/dm^3 s; A_2: the concentration of ETSO at the time of t.

Infrared spectroscopic analysis of HTSO, ETSO, ETSO-PEA and ATSO

The infrared spectrum of HTSO, ETSO, ETSO-PEA and ATSO is shown in Fig. 3a. In the infrared spectrum of HTSO, the absorption peaks that occur at 800 cm^{-1} represent the Si-C stretching vibration peak and those around 1098 and 1019 cm^{-1} represent the stretching vibration absorption peaks of the main chain Si–O–Si. The absorption peaks at 1262 cm^{-1} belong to the plane rocking vibration peak of the –CH_3 in Si-CH_3, and those around 2963 and 2905 cm^{-1} represent –CH_3 asymmetric stretching vibration peaks. Furthermore, the absorption peaks occurring at 2130 cm^{-1} belong to the Si–H absorption peak, which indicate that D4 has participated in the ring-opening polymerization reaction and Si–H bond was successfully introduced into the product.

In the infrared spectrum of ETSO, the absorption peaks that occur at 800 cm^{-1} represent the Si–C stretching vibration peak and those around 1098 and 1016 cm^{-1} represent the main chain Si–O–Si stretching vibration peak. But it is worth noting that the stretching vibration peaks of ether linkage C–O–C that occur around 1106 cm^{-1} are overlapped with Si–O–Si stretching vibration peaks. And those

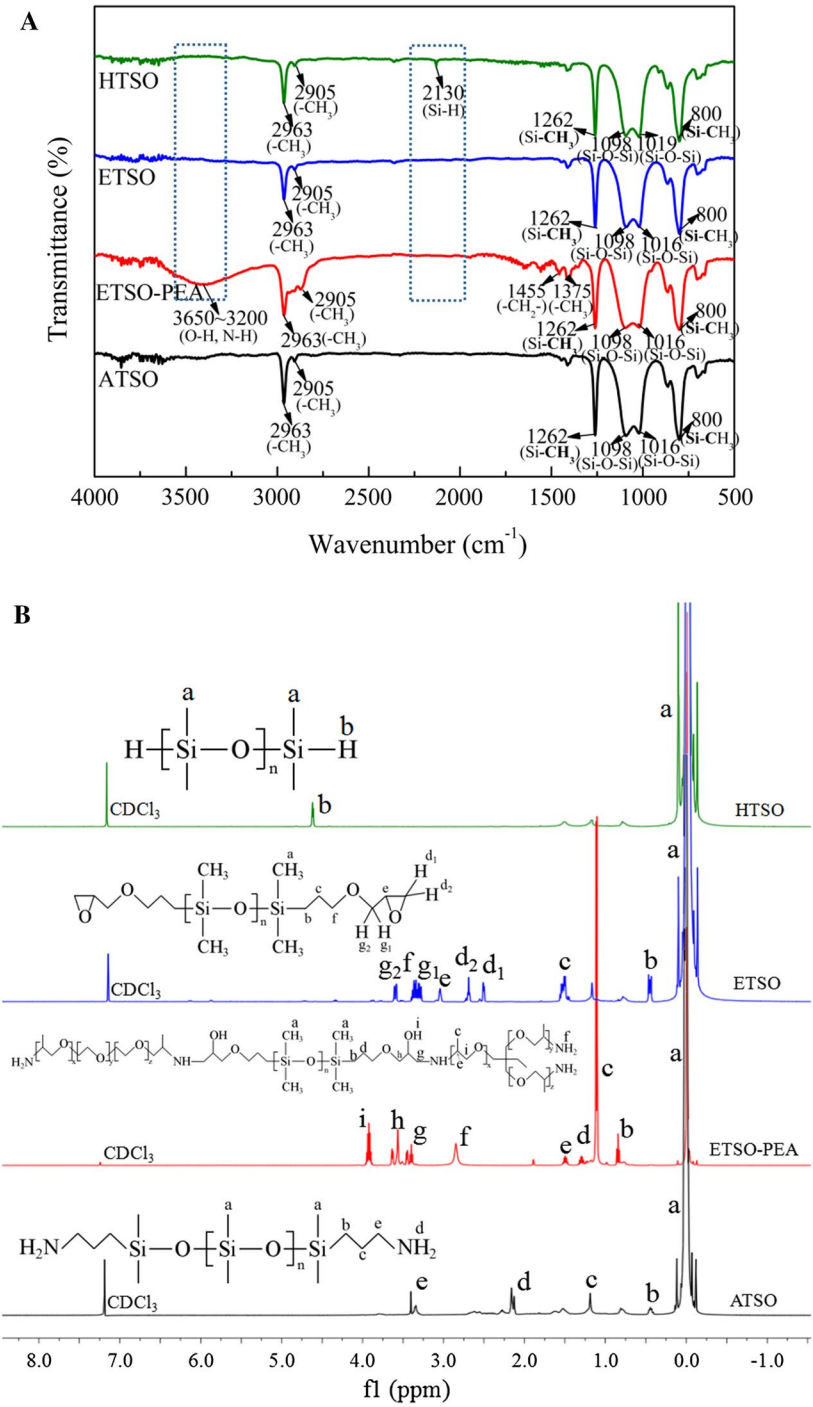

Fig. 3 Infrared spectrum (**a**) and ^{1}H NMR spectrum (**b**) of HTSO, ETSO, ETSO-PEA and ASTO

absorption peaks at 2963 and 2905 cm^{-1} represent the asymmetric stretching vibration peak of $–CH_3$, which show that the structure of main bond was preserved in the hydrosilylation reaction. Besides, the Si–H and C=C absorption peak around 2130 and 1647 cm^{-1} (Fig. S1) disappeared, which indicate that Si–H and C=C were adequately reacted.

In the infrared spectrum of ETSO-PEA, the absorption peaks that occur at 800 cm^{-1} represent the Si–C stretching vibration peak and those at 1262 cm^{-1} belong to the plane rocking vibration peak of $–CH_3$ in Si-CH_3. The absorption peaks around 1455–1375 cm^{-1} represent $–CH_2–$ and $–CH_3$ stretching vibration peaks, respectively. The absorption peaks around 3650–3200 cm^{-1} represent N–H stretching vibration peaks of primary amines and O–H stretching vibration peaks, which were from the reaction of ETSO and polyether amines (T403 and ED600). Compared to T403 and ED600, the amine group absorption peaks had become weaker in ETSO-PEA and such peaks were not present in the infrared spectrum of ETSO (Fig. S1), which indicate that the amine groups had reacted and the epoxy ring-opening reaction had occurred. There existed Si–O–Si stretching vibration peaks at 1098 and 1016 cm^{-1} as well as the asymmetric stretching vibration peaks of $–CH_3$ at 2963 and 2905 cm^{-1}, which indicate that the main structure of the previous product had been retained.

In the infrared spectrum of ATSO, the absorption peaks that occur around 1098 and 1016 cm^{-1} represent the main chain Si–O–Si stretching vibration peak. The absorption peaks at 1262 cm^{-1} belong to the plane rocking vibration peak of $–CH_3$ in Si-CH_3 and those around 2963 and 2905 cm^{-1} represent $–CH_3$ asymmetric stretching vibration peaks.

In conclusion, the infrared spectrum indicates that the main functional groups (Si–O–Si, N–H, C–O–C, O–H, etc.) have been introduced into the structure of the final product ETSO-PEA.

^{1}H NMR analysis of HTSO, ETSO, ETSO-PEA and ATSO

The ^{1}H NMR spectrum of HTSO, ETSO, ETSO-PEA and ATSO is shown in Fig. 3b. The ^{1}H NMR analysis data are listed in order:

HTSO, ^{1}H NMR (δ, ppm, 500 MHz, $CDCl_3$): $\delta_{-0.12\sim0.12}$ (m, SiC**H**$_3$, 984H), $\delta_{4.62\sim4.65}$ (m, Si**H**, 2H).

ETSO, ^{1}H NMR (δ, ppm, 500 MHz, $CDCl_3$): $\delta_{-0.12\sim0.12}$ (m, SiC**H**$_3$, 984H), $\delta_{0.45\sim0.49}$ (m, SiC**H**$_2$, 4H), $\delta_{1.47\sim1.58}$ (m, SiCH$_2$C**H**$_2$, 4H), $\delta_{2.52\sim2.54}$ (m, CHOC**H**$_2$, 2H), $\delta_{2.71\sim2.73}$ (m, CHOC**H**$_2$, 2H), $\delta_{3.05\sim3.08}$ (m, C**H**OCH$_2$, 2H), δ 3.30–3.35 (m, OC**H**$_2$CH, 2H), δ 3.37–3.43 (m, OC**H**$_2$CH$_2$, 2H), δ 3.61–3.65 (m, OC**H**$_2$CH, 2H).

ETSO-PEA, ^{1}H NMR (δ, ppm, 500 MHz, $CDCl_3$): $\delta_{-0.12\sim0.12}$ (m, SiC**H**$_3$, 984H), $\delta_{0.84\sim0.87}$ (m, SiC**H**$_2$, 4H), $\delta_{1.11\sim1.19}$ (m, CHC**H**$_3$, 42H), $\delta_{1.27\sim1.34}$ (m, SiCH$_2$C**H**$_2$, 4H), $\delta_{1.48\sim1.53}$ (m, C**H**CH$_3$, 4H), $\delta_{2.85\sim2.98}$ (m, CHN**H**, 8H), $\delta_{3.39\sim3.42}$ (m, C**H**$_2$NH, 4H), $\delta_{3.45\sim3.47}$ (m, OC**H**$_2$CH, 12H), $\delta_{3.90\sim3.95}$ (m, CHO**H**, 2H).

ATSO, ^{1}H NMR (δ, ppm, 500 MHz, $CDCl_3$): $\delta_{-0.12\sim0.12}$ (m, SiC**H**$_3$, 996H), $\delta_{0.41\sim0.46}$ (m, SiC**H**$_2$, 4H), $\delta_{1.19}$ (s, SiCH$_2$C**H**$_2$, 4H), $\delta_{2.13\sim2.16}$ (m, CH$_2$N**H**$_2$, 4H), $\delta_{3.34\sim3.41}$ (m, C**H**$_2$NH$_2$, 4H).

In summary, the data indicate that the chemical structure of the final product ETSO-PEA was confirmed, which is consistent with the expected structure.

Thermal gravimetric analysis

The cotton fabrics treated with silicones need to cure at 180 °C; thus, the silicones should exhibit good thermal stability. The thermograms and the corresponding DTG curves of ETSO-PEA and ATSO are shown in Fig. 4. The decomposition temperature of ETSO-PEA ranged from 205 to 280 °C, lower than the ATSO samples with a range from 250 to 400 °C, which could be attributed to the high-temperature fracture of ether bonds in ETSO-PEA. The results show that ETSO-PEA and ATSO both express a good thermal stability that means they can be applied onto the cotton fabrics at elevated temperature.

Application of ETSO-PEA solution to cotton fabrics

Particle size of emulsion

Amino silicones are currently the most widely used for the functional finishing. The silicones are generally prepared into microemulsion, with a particle size of about 50–150 nm [19, 34, 35]. The positively charged emulsions can be strongly adsorbed on the surface of negatively charged cotton fabrics. Thus, a lower concentration of the solution can lead to a higher molecular distribution and a higher adsorption [36]. The structure of silicone molecules and the introduced functional groups determine the surface modification properties of the cotton fabric [37]. Figure 5a, b shows that the particle size of the dispersed phase in the emulsion of ETSO-PEA and ATSO is basically distributed between 10–150 and 10–400 nm, respectively. And the solution emulsified was blue fluorescent and transparent. But, the particle size of the solution with only AEO-7 and HAc was very large, more than 1000 nm, and the solution was cloudy (Fig. 5c). Thus, it was further confirmed that amino silicone oil contributes to the formation of microemulsions.

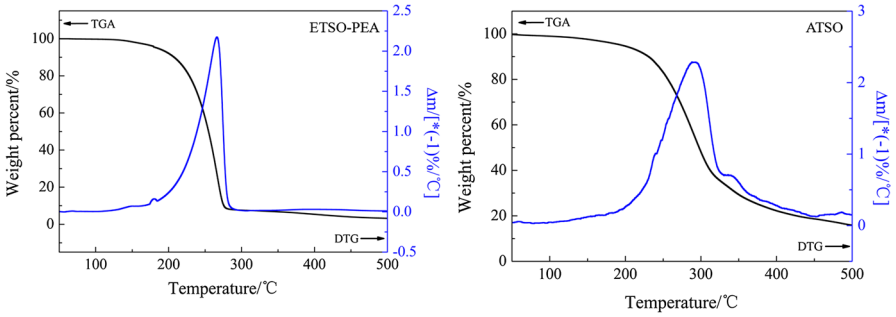

Fig. 4 TGA and DTG curves of ETSO-PEA and ATSO

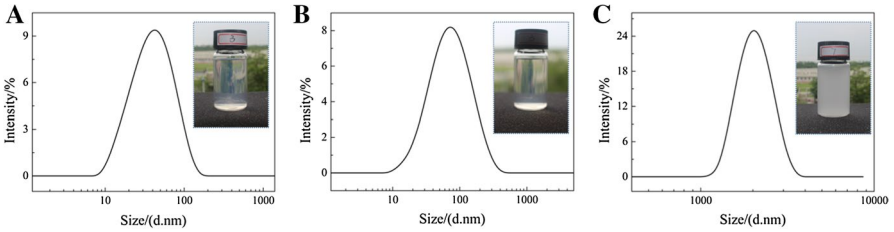

Fig. 5 The distribution of particle size of silicone emulsion, **a** ETSO-PEA (30 g/L); **b** ATSO (30 g/L); **c** the mixed solution of AEO-7 and HAc (without silicone)

Micromorphology observation and physical tests of as-prepared cotton fabrics

The morphological structure of untreated, ETSO-PEA- and ATSO-treated cotton fabrics was observed by using SEM (Fig. 6). The surface of untreated cotton fabrics (Fig. 6a) was much rougher than the other two treated samples, and there were more scales and clearance on the surface. After treating the fabric samples with the solution of silicones, a thin smooth film was coated on the surface of fibers, as well as the fiber clearance and folds were blocked (Fig. 6b, c). What is more, the surface of the whole fabric was neat and smooth, compared to the untreated samples. Meanwhile, bending rigidity (BR) of the untreated and treated cotton fabrics was also measured (Table 3). A lower bending rigidity (BR) value represents a better softness. The results show that the macroscopic surface roughness of cotton fabrics is in accordance with the micromorphological structure of untreated, ETSO-PEA- and ATSO-treated cotton fabrics. The ETSO-PEA-treated cotton fabrics expressed a lower BR value than the untreated samples, but slightly higher than the ATSO-treated samples. This was attributed to the continuous and sequentially oriented Si-CH_3 groups helping to increase the softness of fabrics with the primary amine as a terminal group, but the polyether segments in ETSO-PEA disrupting the continuous neatly arranged Si-CH_3 groups limited the movement of polysiloxane segment. It was also found that the whiteness of ETSO-PEA (30 g/L)-treated cotton fabrics remained similar to the untreated raw samples. Compared with the other two samples, a slight yellowing of the fabrics occurred after treating with ATSO. Thus, this kind of terminal amino silicone was more suitable for dark fabric finishing.

Water contact angles

There are many hydroxyl groups on the cotton fabrics, so that the untreated fabrics have a good hydrophilicity and short water absorption time, only about 0.046 s (Table 3). ATSO-treated cotton fabrics have a long static water absorption time about 52.0 s (Fig. 7), more than twice as much as ETSO-PEA-treated fabrics. At the time of 20 s, the static water has completely spread out on the untreated and ETSO-PEA-treated fabrics, but it still maintained a complete drop of water on the ATSO-treated samples. The introduction of polyether groups in ETSO-PEA increased

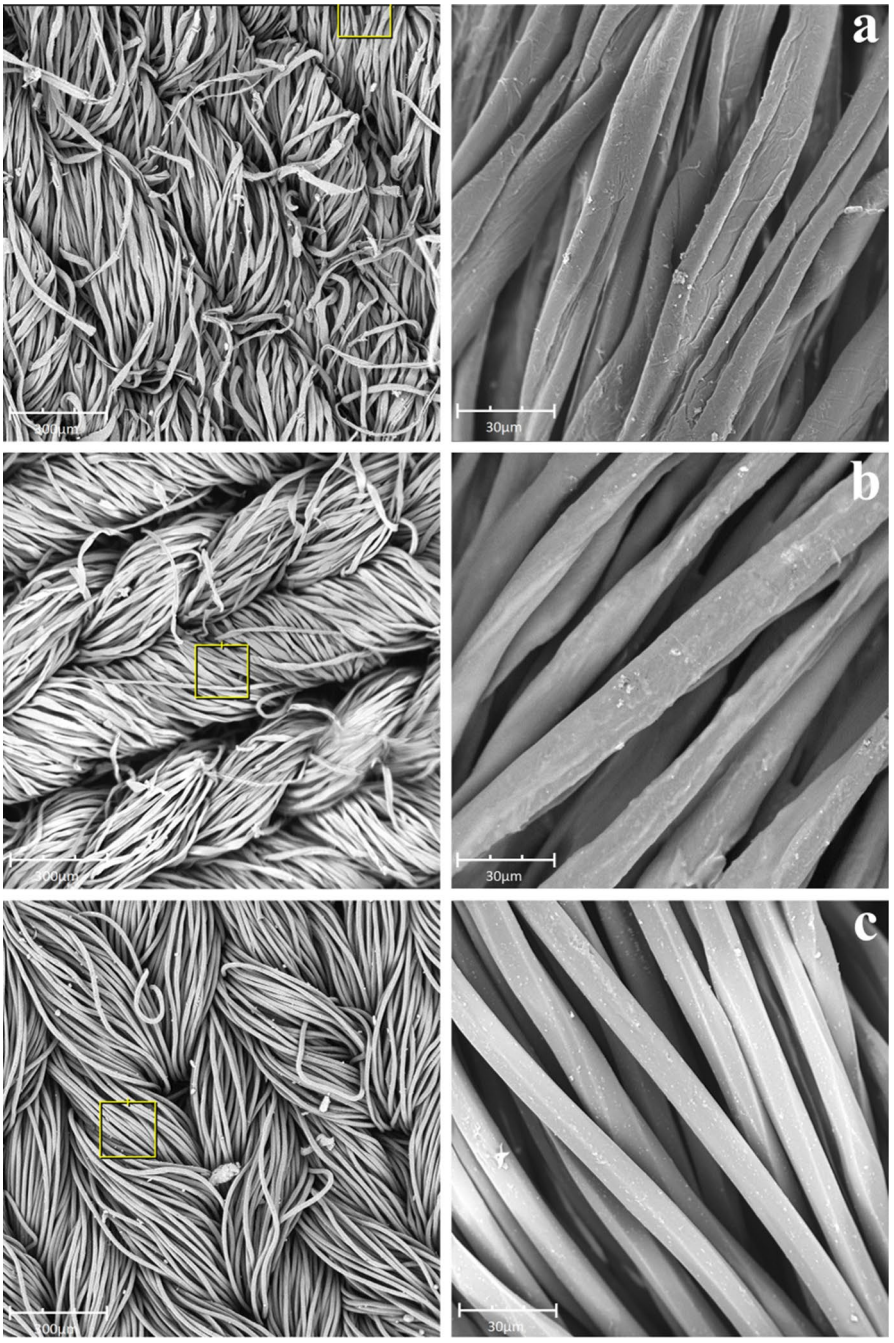

Fig. 6 Scanning electron microscopy photographs of untreated and treated cotton fabrics: **a** raw samples; **b** ETSO-PEA/cot; **c** ATSO/cot

Table 3 Physical–mechanical properties of raw sample, ETSO-PEA- and ATSO-treated cotton fabrics

	Whiteness index (°)	Bending rigidity (mN)	Static water absorption time (s)
Raw sample	69.3	424	0.046
ETSO-PEA/cot (30 g/L)	66.4	386	20.0
ATSO/cot (30 g/L)	58.1	358	52.0

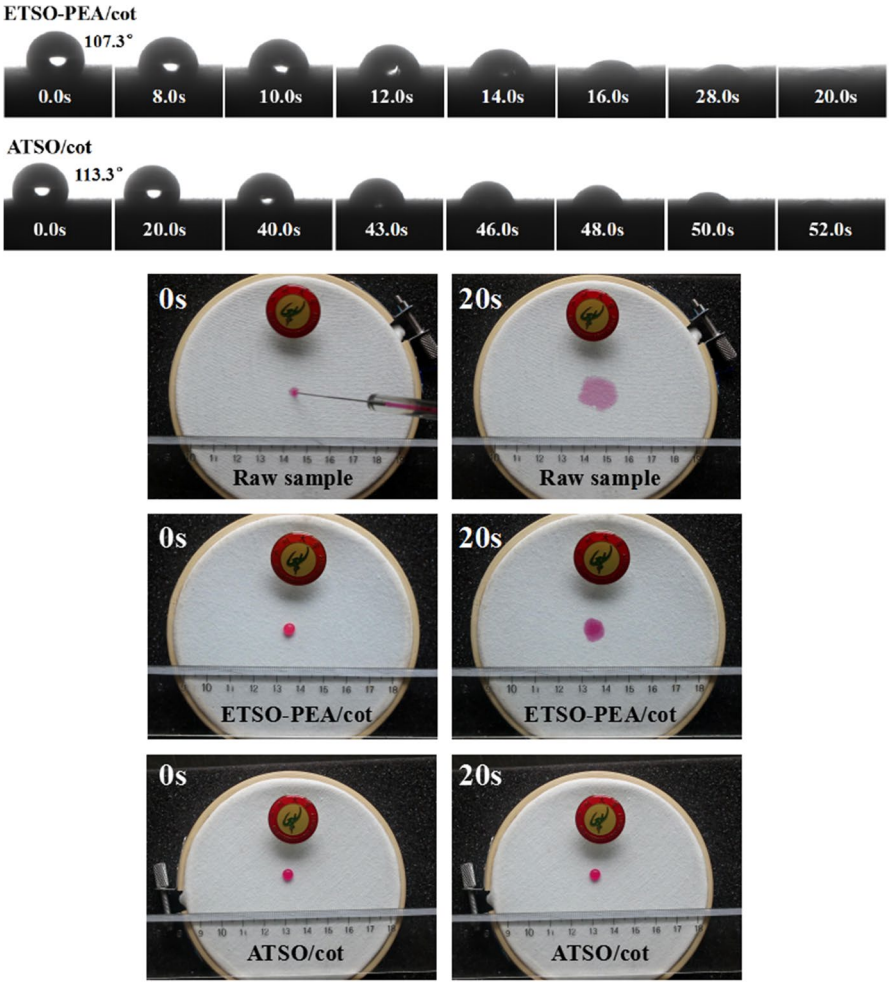

Fig. 7 Water contact angles and static water absorption time of raw samples, ETSO-PEA/cot and ATSO/cot

the hydrophilicity and wettability of the fabrics, compared with the ATSO-treated samples.

Molecular interaction model of the softener on the fabrics

Amino silicone softener was fixed onto the cotton fabrics, and the surface was modified with the formation of a network structure. Meanwhile, the extent of networking and crosslinking enhanced a lot, which provided a good soft handle [38].

The location and arrangement of functional groups in the silicone molecules have a great influence on the hydrophilicity of the treated cotton fabrics. The corresponding proposed schematic model is described in Fig. 8. With a low surface tension, polysiloxane molecules could more easily spread and closely cover the surface of cotton fabrics [39, 40]. In microscopic view, it could be proposed that via electrostatic interactions and hydrogen bonding, the polarized Si–O groups and protonated amino groups are tightly attached to the negatively charged cotton fabrics [14, 41, 42].

Based on the results which were presented in a previous paper [16], it could be proposed, for ATSO-treated cotton fabrics, that the entire polysiloxane segment was anchored on the surface of cotton fabrics via the amino groups, a ring of polysiloxane segments between two amino groups was free to form and Si–CH_3 groups were arranged orderly on the surface of fabrics (Fig. 8a). Because of the easy movement and easy bending of the ring segment, the friction coefficient between the fibers was reduced, and the cotton fabrics became soft and smooth (Fig. 8b). However, for the ETSO-PEA-treated samples, the softness of the fabrics was slightly reduced because the polyether segment with less bending disrupted the continuous neatly arranged Si–CH_3 groups and limited the movement of the polysiloxane segment (Fig. 8c). Meanwhile, the hydrophilic polyether groups could form a hydrophilic layer on the surface of fibers [16]. Thus, water could more easily spread on the ETSO-PEA-treated fabrics than on the ATSO-treated samples. Furthermore, in a dry state, cyclic polysiloxane segments were on the outermost layer of the fiber surface and the polyether segments were lodged or bent on the surface of fiber; in a wet state, the position of cyclic polysiloxane segments and polyether segments was exactly opposite (Fig. 8d). So, ETSO-PEA-treated cotton fabrics showed good softness in the dry state and fine hydrophilicity in wet state.

Conclusions

A multiblock linear polyether functional amino silicone softener (ETSO-PEA) was synthesized by using a three-step reaction pathway. Single-factor (reaction time, reaction temperature and catalyst concentration) and orthogonal array design experiments were carried out to investigate the optimal reaction conditions. In the first two steps, the data between viscosity/conversion rate and reaction time showed that the two steps were both kinetic first-scale reaction, and the kinetic equation was: $r_1 = 0.18$ [A_1] and $r_2 = 0.67$ [A_2]. The silicones were used as softeners to modify the

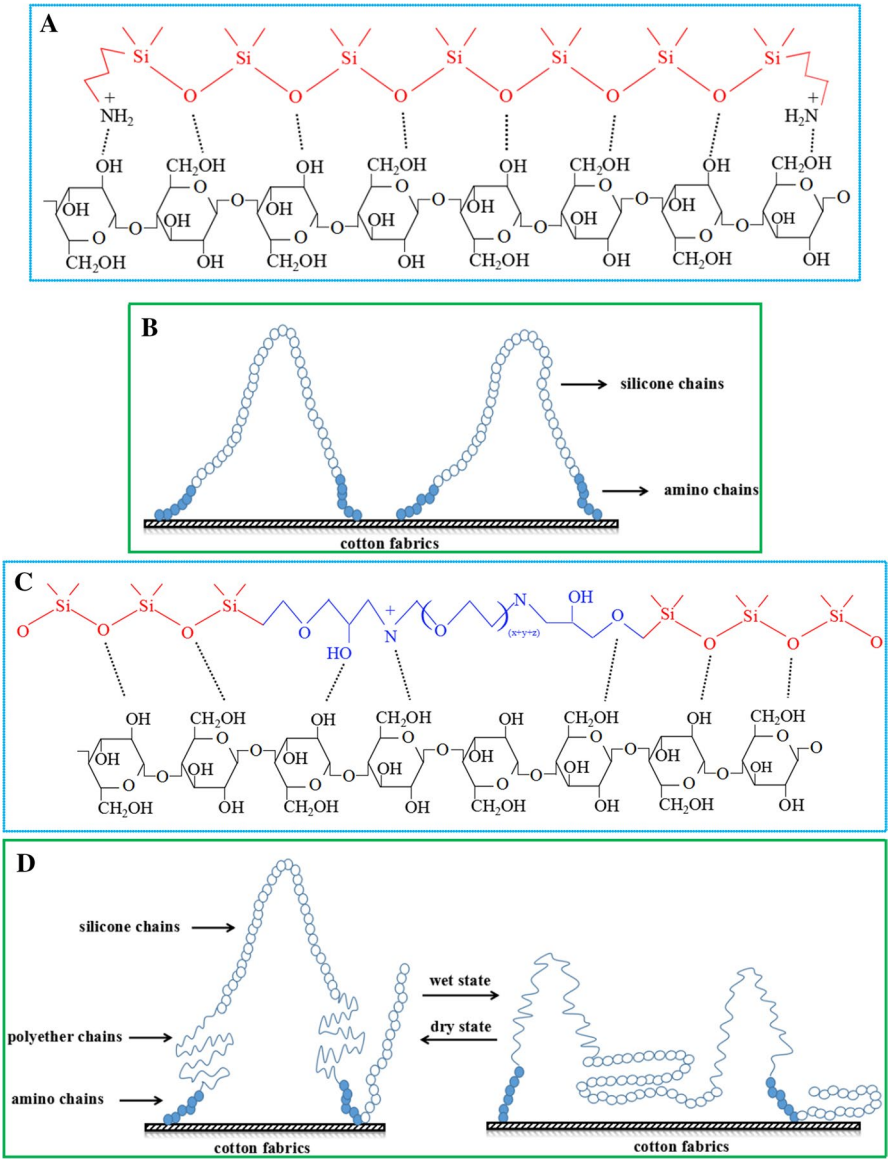

Fig. 8 The structure of amino silicones and proposed schematic model for silicones adsorbed on the cotton fabrics: **a** ATSO; **b** ATSO-treated fabrics; **c** ETSO-PEA; **d** ETSO-PEA-treated fabrics

surface of cotton fabrics, and the results indicated that the ETSO-PEA-treated cotton fabrics expressed better whiteness than traditional ATSO-treated samples. SEM images showed that the ETSO-PEA- and ATSO-treated cotton fabrics could significantly improve smoothness of the surface compared with the untreated samples. The water contact angles and static water absorption time showed that the introduction

of polyether groups in ETSO-PEA increased the hydrophilicity and wettability of the fabrics, compared with the ATSO-treated samples.

Such differences between ETSO-PEA- and ATSO-treated cotton fabrics could be attributed to the molecular structure of silicones and their arrangement on the surface of fabrics. It was found that the introduction of polyether groups can enhance the hydrophilicity and wettability of the fabrics, but slightly reduce the softness. It was proposed that the polyether segment with less bending disrupted the continuous and sequentially oriented Si-CH_3 groups and limited the movement of the polysiloxane segment. In addition, the functional silicone softener that can improve comprehensive performance properties (such as good softness, smoothness, wettability and hydrophilicity) of the fabrics should be researched and developed constantly to match the customer perception.

Acknowledgements We gratefully acknowledged the support of the National Science Foundation of China Project (No. 21676061).

References

1. Zuber M, Zia KM, Tabassuma S, Shazia T, Jamil T, Barkaat-ul-Hasin S, Khosa MK (2011) Preparation of rich handles soft cellulosic fabric using amino silicone based softener, part II: color-fastness properties. Int J Biol Macromol 49:1–6
2. Hauser PJ, Smith CB, Hashem MM (2004) Ionic crosslinking of cotton. Autex Res J 4(2):95–100
3. Xu YJ, Yin H, Yuan SF, Chen ZR (2009) Film morphology and orientation of amino silicone adsorbed onto cellulose substrate. Appl Surf Sci 255:8435–8442
4. Hou AQ, Chen S (2009) Preparation of microemulsions of the polysiloxanes modified with different amines and their effect on the color shade of dyed cellulose. J Dispers Sci Technol 31:102–107
5. Hou AQ, Shi YQ (2009) Polymerization and surface active properties of water-soluble amphiphilic polysiloxane copolymers modified with quaternary ammonium salts and long-carbon chain groups. Mater Sci Eng B 163:99–104
6. Xie KL, Chen Y, Hou AQ, Shi YQ (2009) Preparation and properties of the emulsions of the polysiloxane material modified with tertiary amino side chain. J Dispers Sci Technol 30:1474–1480
7. Noll W (1968) Chemistry and technology of silicones. Academic Press, New York
8. An Q, Wang Q, Li L, Huang L (2009) Study of amino functional polysiloxane film on regenerated cellulose substrates by atomic force microscopy and X-ray photoelectron microscopy. Text Res J 79:89–93
9. Mohamed AL, Er-Rafik M, Moller M (2013) Suitability of confocal raman microscopy for monitoring the penetration of PDMS compounds into cotton fibres. Carbohydr Polym 96:305–313
10. Skinner MW, Qian C, Grigoras S, Halloran DJ, Zimmerman BL (1999) Fundamental aspects of aminoalkyl siloxane softeners by molecular modeling and experimental methods. Text Res J 69(12):935–943
11. Wang WZ, Lu YQ, Cai ZY (2010) Study on surface characters of methylsioxane-oxyalkylene copolymers. Fine Chem 27(3):229–233
12. Fouda MMG, Fahmy HM (2011) Multifunctional finish and cotton cellulose fabric. Carbohydr Polym 86:625–629
13. Kang TJ, Kim MS (2001) Effects of silicone treatments on the dimensional properties of wool fabric. Text Res J 71(4):295–300
14. Xu Y, Hong Y, Yuan S, Chen Z (2009) Film morphology and orientation of amino silicone adsorbed onto cellulose substrate. Appl Surf Sci 255(20):8435–8442

15. Avinc O, Wilding M, Phillips D, Farrington D (2010) Investigation of the influence of different commercial softeners on the stability of poly(lactic acid) fabrics during storage. Polym Degrad Stab 95(2):214–224
16. Yu FJ, Qun P, Hong F (2015) Synthesis of linear piperazine/polyether functional polysiloxane and its modification of surface properties on cotton fabrics. ACS Appl Mater Interfaces 7(14):7552–7558
17. Purohit PS, Kulkarni R, Somasundaran P (2012) Investigation of colloidal properties of modified silicone polymers emulsified by non-ionic surfactants. J Colloid Interface Sci 383:49–54
18. Nguyen L, Hang M, Wang W, Tian Y, Wang L, McCarthy TJ, Chen W (2014) Simple and improved approaches to long-lasting, hydrophilic silicones derived from commercially available precursors. ACS Appl Mater Interfaces 6:22876–22883
19. Zia KM, Tabassum S, Barkaat-Ul-Hasin S, Zuber M, Jamil T, Jamal MA (2011) Preparation of rich handles soft cellulosic fabric using amino silicone based softener. Part-I: surface smoothness and softness properties. Int J Biol Macromol 48(3):482–487
20. Xu YJ, Yin H, Zheng HF, Yuan SF, Chen ZR (2011) Application performance and surface morphologies of amino polysiloxanes with different amino values and amino types. J Appl Polym Sci 119:2326–2333
21. Li MT, An QF, Huang LX (2008) Film morphology and orientation of *N*-cyclohexyl-γ-aminopropyl polydimethylsiloxane. Surf Interface Anal 40:914–918
22. Xu C, Ouyang L, Liu H, Chen Q, Cai Z, Xing J (2015) Synthesis of blocking polyether silicone oil and silicone blocking waterborne polyurethane and application to cashmere knitted fabric finishing. Text Res J 85(19):1–10
23. Habereder P, Bereck A (2002) Silicone softeners. Rev Prog Color 32:125–137
24. An QF, Yang G, Wang QJ, Huang LX (2008) Synthesis and morphology of carboxylated polyether-block-polydimethylsiloxane and the supermolecule self-assembled from it. J Appl Polym Sci 110:2595–2600
25. An QF, Zhao J, Li XQ, Wei YB, Qin W (2014) Synthesis of dimethyldodecyl quaternary ammonium polyether polysiloxane and its film morphology and performance on fabrics. J Appl Polym Sci 131(16):40613–40619
26. Chung DW, Lim JC (2009) Study on the effect of structure of polydimethylsiloxane grafted with polyethyleneoxide on surface activities. Colloid Surface A 336:35–40
27. Wu X, Leung DYC (2011) Optimization of biodiesel production from camelina oil using orthogonal experiment. Appl Energ 88(11):3615–3624
28. Geck M, Lautenschlager H, Deubzer B, Stinglhammer P, Habereder P, Ullrich K (1998) Preparation of organopolysiloxane microemulsions. US, US5712343
29. Min CN, Pu Q, Yang L, Fan H (2014) Synthesis, film morphology, and performance on cotton substrates of dodecyl/piperazine functional polysiloxane. J Appl Polym Sci 131(8):498–505
30. Vilanova N, Rodríguez-Abreu C, Fernandez-Nieves A, Solans C (2013) Fabrication of novel silicone capsules with tunable mechanical properties by microfluidic techniques. ASC Appl Mater Interfaces 5(11):5247–5252
31. Mourey TH, Turner SR, Rubinstein M, Frechet JMJ, Hawker CJ, Wooley KL (1992) Unique behavior of dendritic macromolecules: intrinsic viscosity of polyether dendrimers. Macromolecules 25(9):2401–2406
32. Stanley RS, Ler JAB (1998) Polymer synthesis and characterization. Polymer synthesis and characterization: a laboratory manual. Academic Press, vol 277, no 2–3, pp 115–122
33. Schramm C, Rinderer B, Tessadri R (2014) Non-formaldehyde, crease resistant agent for cotton fabrics based on an organic-inorganic hybrid material. Carbohydr Polym 105(1):81–89
34. Kulkarni R, Deshpande A, Kushare B (2001) Silicones for textile finishing. Colourage 48(2):21–27
35. Abo-Shosha MH, Hashem AM, El-Hosamy MB, El-Nagar AH (2008) Easy care finishing of knitted cotton fabric in presence of a reactive-type antibacterial agent. J Ind Text 38(2):103–126
36. Habereder P, Bereck A (2002) Silicone softeners: structure-effect-relationship. Rev Prog Color Relat Top 32:125–137
37. Montazer M, Hashemikia S (2012) Application of polyurethane/citric acid/silicone softener composite on cotton/polyester knitted fabric producing durable soft and smooth surface. J Appl Polym Sci 124(5):4141–4148
38. Mohamed H, Nabila I, Amira ES, Rakia R, Peter H (2009) An eco-friendly-novel approach for attaining wrinkle-free/soft-hand cotton fabric. Carbohydr Polym 78(4):690–703

39. Ozcam AE, Spontak RJ, Genzer J (2014) Toward the development of a versatile functionalized silicone coating. ASC Appl Mater Interfaces 6(24):22544–22552
40. Svensson AV, Johnson ES, Nylander T, Piculell L (2010) Surface deposition and phase behavior of oppositely charged polyion-surfactant ion complexes. 2. A means to deliver silicone oil to hydrophilic surfaces. ACS Appl Mater Interfaces 2(1):143–156
41. Burrell Michael C, Butts Matthew D, Derr Daniel (2004) Angle-dependent XPS study of functional group orientation for aminosilicone polymers adsorbed onto cellulose surfaces. Appl Surf Sci 227(1):1–6
42. Bereck A, Riegel D, Matzat A, Habereder P, Lautenschlager H (2001) Silicones on fibrous substrates: their mode of action. AATCC Rev 1:45–49